

Modeling quaternary ammonium compound inhibition of biological nutrient removal activated sludge

Daniela Conidi, Mehran Andalib, Christopher Andres, Christopher Bye, Art Umble and Peter Dold

ABSTRACT

Quaternary ammonium compounds (QACs) are surface-active organic compounds common in industrial cleaner formulations widely used in various sanitation applications. While acting as effective pathogenic biocides, QACs lack selective toxicity and often have poor target specificity. As a result, adverse effects on biological processes and thus the performance of biological nutrient removal (BNR) systems may be encountered when QACs enter wastewater treatment plants (WWTPs). Because of these impacts, there is motivation to screen wastewater influents for QACs and for process engineers to consider the inhibition effects of QACs on process evaluation and design of BNR plants. This paper introduces a mathematical model to describe the fate of QACs in a WWTP via biodegradation and bio-adsorption, and the inhibitory effect of QACs on nitrifiers and ordinary heterotrophic organisms. The model was incorporated as an add-on model in BioWin 5.3 and simulations of experimental systems were used for comparison of model results to measured data reported in the literature. The model was found to accurately predict the bulk phase concentration of QAC and the inhibition of nitrification with QAC concentrations ≥ 2 mg/L. This work provides a preliminary framework for simulation of BNR plants receiving inhibitory substances in the influent.

Key words | BNR, inhibition, modeling, quaternary ammonium compounds

Daniela Conidi
Christopher Bye
Peter Dold
Envirosim Associates Ltd,
175 Longwood Rd S, Suite 114A, Hamilton, ON L8P
0A1,
Canada

Mehran Andalib (corresponding author)
Christopher Andres
Art Umble
Stantec Inc.,
Edmonton, AB T5 K 2L6,
Canada
E-mail: mehran.andalib@stantec.com

INTRODUCTION

Quaternary ammonium compounds (QACs) are used extensively in domestic, agricultural, health care, and industrial applications as surfactants, emulsifiers, fabric softeners, disinfectants, pesticides, corrosion inhibitors, paint additives, cosmetics and personal care products (Yang *et al.* 2014). In 2004, global annual consumption of QACs was estimated at 500,000 tons and increasing (Chen *et al.* 2018). The widespread use of QACs means that they may be present in many wastewater treatment plant (WWTP) influents. It has been reported that roughly 75% of all QACs consumed end up in influent to WWTPs (Carbajo *et al.* 2015). QAC concentrations in the range of 25–300 mg/L, 0.3–3.6 mg/L and 22–103 mg/kg have been reported in the influents, effluents, and sludges of WWTPs, respectively (Ruan *et al.* 2014; Carbajo *et al.* 2015; Khan *et al.* 2015; Zhang *et al.* 2015). In addition, mean concentrations of 3,700 mg/kg have been reported in the sludge from five WWTPs in Switzerland (Zhang *et al.* 2015).

doi: 10.2166/wst.2018.449

QACs are composed of at least one hydrophobic hydrocarbon chain linked to a positively charged nitrogen atom, and other alkyl groups which are mostly short-chain substituents such as methyl or benzyl groups. This structure gives them unique physical and chemical properties (Ren *et al.* 2011). While acting as effective biocides against a wide range of pathogenic microorganisms, QACs lack selective toxicity and often have poor target specificity. As a result, they negatively impact the physiological groups responsible for wastewater treatment and thus the performance of biological nutrient removal (BNR) systems. For example, QACs have been found to inhibit respiratory enzymes decreasing the rate of chemical oxygen demand (COD) substrate utilization (Zhang *et al.* 2010). QACs also have an adverse effect on nitrification. Total inhibition of nitrification was found at a QAC concentration of 2 mg/L due to enzymic toxicity (Sütterlin *et al.* 2008), while a QAC concentration greater than 50 mg/L has been reported to inhibit

heterotrophic denitrification, with low temperatures exacerbating the inhibitory effect on nitrite reduction (Hajaya 2011; Yang et al. 2014). In addition, a QAC concentration of 50 mg/L was found to affect anaerobic degradation resulting in reduced methane production and volatile fatty acid accumulation (Tezel 2009).

It has been reported in the literature that the most effective method for removal of QACs in a treatment facility is through adsorption processes, including adsorption to activated sludge biomass (Ren et al. 2011). The tendency for QACs to adsorb onto solids and accumulate in the WWTP has been shown to increase with increased alkyl chain length. QAC sorption also is strongly related to temperature, with decreasing temperature resulting in an increased sorption rate onto activated sludge (Zhang et al. 2015). Equilibrium partitioning data between the solid and liquid phase have been described well by both Langmuir and Freundlich isotherm models (Ren et al. 2011). Adsorption kinetics have been best described by a pseudo-second-order model (Ren et al. 2011). Higher initial concentrations in the bulk liquid increase the adsorption capacity (Chen et al. 2018).

Another QAC removal mechanism is biodegradation. QACs are considered to be biodegradable upon complete depletion of available readily and slowly biodegradable COD (Zhang et al. 2010). Since QACs also inhibit respiration and hence COD utilization, respiratory inhibition is also responsible for the fate of QACs in activated sludge. In addition, microbial acclimation and enrichment has been shown to contribute to reduced inhibition and enhanced biodegradation of QACs in laboratory-scale BNR systems (Hajaya & Pavlostathis 2012).

As a result of the negative impacts of QACs on biological treatment systems, there is motivation to screen wastewater influents for QACs and for process engineers to consider the inhibition effects of QACs on process evaluation and design of BNR plants. Designs should provide adequate mixed liquor levels for proper adsorption of QACs and biodegradation to below the nitrifier inhibitory threshold. The objectives of the present study are to:

- (1) introduce a mathematical model to simulate the different degrees of QAC inhibition of nitrifiers (ammonia- and nitrite-oxidizers, AOB, NOBs) and ordinary heterotrophic microorganisms (OHOs) at different operational conditions;
- (2) enhance the understanding of the fate and effect of QACs in engineered treatment systems, in turn contributing to the effective design and management of QAC-containing wastewaters; and

- (3) provide an effective framework for proper simulation and design of a WWTP with inhibitory substances.

MATERIALS AND METHODOLOGY

Literature data

The present study leveraged data and observations from two key sources:

- (1) Hajaya, M. 2011 *Fate and Effect of Quaternary Ammonium Antimicrobial Compounds on Biological Nitrogen Removal within High-Strength Wastewater Treatment Systems*. PhD Thesis, Georgia Institute of Technology, Atlanta, GA, USA.
- (2) Yang, J., Tezel, U., Li, K. & Pavlostathis, S. G. 2014 Prolonged exposure of mixed aerobic cultures to low temperature and benzalkonium chloride affect the rate and extent of nitrification. *Bioresource Technology*, **179**, 193–201.

Hajaya (2011)

Hajaya assessed and quantified the inhibitory effect of QACs and evaluated the role of adsorption, inhibition, and biodegradation on the fate and effect of QACs in a BNR system treating poultry-processing wastewater. Figure 1 illustrates the continuous flow BNR system, which included pre-anoxic, anoxic, and aerobic reactors with volumes of 4, 4, and 5 L, respectively. The settler volume was 1.5 L. Reactors 1 and 2 were mechanically mixed while mixing in reactor 3 was accomplished via diffused aeration. Raw wastewater was fed at a rate of 2.0 L/day at 4 °C. The temperature in the process was maintained at 22 °C. Total design, actual anoxic, and actual aerobic solids retention times (SRTs) were 25, 10.4, and 12.6 days, respectively. The WAS and nitrate return flow rates were 0.35 and 4.0 L/day, respectively. Target MLSS was 1,200 mg/L and the mixed-liquor target pH was 7.0. The target dissolved oxygen (DO) in

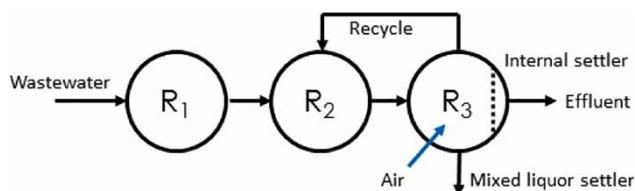


Figure 1 | Process flow diagram of simulated continuous-flow multi-stage BNR system.

the aerobic zone (reactor 3) was 3–5 mg/L, resulting in an airflow of 3–6 m³/h.

The influent poultry processing wastewater TSS, VSS, TCOD, sCOD, NH₃-N, and TN concentrations were 125 mg/L, 120 mg/L, 1,275 mg/L, 919 mg/L, 46 mg N/L and 103 mg N/L, respectively. A blend of three benzalkonium chloride (BAC) (the most common QAC found in wastewater) homologs were used in the Hajaya study as follows: 32% C12BAC/40% C14BAC/8% C16BAC/10% ethanol/10% water. The BNR system was operated without any QAC addition for a period of 30 days, with full nitrification and significant denitrification. From days 30 to 80, a concentration of 5 mg/L QAC was injected continuously in the process.

It is noteworthy to mention that during QAC addition, the concentration of QAC in the pre-anoxic zone and aerobic zone did not exceed 0.3 mg/L, which is well below the established inhibitory threshold for nitrifiers. From day 30 to day 381 the concentration of QAC in the influent stream was increased to 60 mg/L in five incremental steps. During this stage, the QAC concentration in the bulk liquid of the aerobic zone increased from 0.3 mg/L to 1.8 mg/L, still below the nitrifier inhibitory threshold concentration in the bulk liquid. As expected, no inhibition of nitrification or denitrification rates was observed. Because QAC concentrations in the bulk liquid were less than 2 mg/L, Hajaya's study has limited value in terms of validating the proposed model's predicted inhibitory effects of QACs on nitrification. However, it does provide a meaningful dataset that can be used for comparison of predicted QAC adsorption and biodegradation.

Yang *et al.* (2014)

Yang *et al.* assessed (1) the effect of QAC concentration on nitrification at room temperature and (2) investigated the combined effects of QAC and prolonged exposure to low temperature on nitrification. This was accomplished by a series of nitrification assays. For the first objective, a series of short-term batch assays was conducted at room temperature with mixed nitrifying culture developed with mixed-liquor from the RM Clayton WWTP in Atlanta, GA, USA. The steady-state MLVSS was 290 mg VSS/L. Five 200 mL samples of the culture were collected, amended with 100 mg N/L NH₄Cl, and aliquots of QAC were added to each to generate initial QAC concentrations of 5, 10, 15, and 20 mg/L. Each of the five samples were continuously aerated and mixed. The concentration of nitrogen species and QACs were measured. Ammonia oxidation at room

temperature (22–24 °C) by a nitrifying culture was inhibited at increasing QAC concentrations. Significant nitrification inhibition was observed as low as 5 mg QAC/L and nitrification essentially ceased at 15 mg QAC/L. No QAC degradation was observed in the short-term assay (96 hours). Data from this part of the Yang *et al.* study were used to validate predicted QAC inhibition of nitrification.

Model development and assumptions

In this work, a mathematical model was developed to incorporate the following processes:

- (1) adsorption of QAC onto biomass via bio-adsorption kinetics;
- (2) inhibition of AOBs, NOBs, OHOs under aerobic and anoxic conditions at different liquid phase QACs thresholds; and
- (3) biodegradation of liquid phase QACs by OHOs under aerobic and anoxic conditions.

The model assumes that microorganisms are already acclimated to QACs; no population shifts or changes in metabolic abilities were modelled with time. It is also assumed that only the liquid phase concentration of QAC was inhibitory (i.e. adsorbed QAC did not have any inhibition impacts).

To develop the biokinetic expressions describing the impact of QAC inhibition on organism (AOB, NOB, OHO) growth rate, various inhibition expressions from the literature were evaluated. The formulation of the inhibition expressions evaluated included an exponential inhibition term proposed in Aiba *et al.* (1968) (Equation (1)), a Monod-type inhibition term (Equation (2)), and a Haldane inhibition term (Equation (3)), where C_i is the concentration of the inhibitory compound (i.e. QAC) and K_i is the inhibition coefficient:

$$\exp^{-\frac{C_i}{K_i}} \quad (1)$$

$$\frac{K_i}{C_i + K_i} \quad (2)$$

$$\frac{C_i}{K_s + C_i + \frac{C_i^2}{K_i}} \quad (3)$$

Based on comparisons to the experimental literature data reported by Hajaya (2011) and Yang *et al.* (2014), the most accurate inhibition model for AOBs and NOBs was found with a Monod-type inhibition expression. Aerobic

and anoxic growth of OHOs on QAC (C_i) was found to be best described using Haldane substrate utilization kinetics. With Haldane kinetics, as the value of the inhibition parameter (K_i) decreases, the degree of inhibition on growth increases. The impact of temperature, limiting nutrient concentrations (e.g. ammonia, phosphate, CO_2 , cations, anions) and pH inhibition were also included in the biokinetic expressions for organism growth.

Adsorption data from the literature were evaluated to determine the appropriate formulation of QAC adsorption onto biomass (i.e. bio-adsorption kinetics). Ren *et al.* (2011) found that equilibrium adsorption of QACs onto activated sludge at 25 °C was best described using a Langmuir isotherm. Adsorption experiments were carried out by Ren *et al.* (2011) with initial QAC concentrations in the range of 10–140 mg/L at 25 °C. The sludge concentration was 250 mg/L and the contact time was 4 h. Adsorption isotherms were also reported at different temperatures; adsorption of QAC onto activated sludge was found to be inversely proportional to temperature. The maximum sorbed QAC concentration (q_{max} , g/g) was extrapolated from the temperature dependent isotherms reported by Ren *et al.* (2011) and a relationship was developed to correct the maximum amount of QAC that can be sorbed for temperature. The following isotherm (Equation (4)) was derived to describe adsorption of QAC onto biomass:

$$q_e = q_{\text{max}} \times 0.988^{(T-15)} \cdot \frac{K_L \cdot C_e}{1 + K_L \cdot C_e} \quad (4)$$

where q_e is the sorbed phase QAC concentration at equilibrium, q_{max} is the Langmuir isotherm constant (reported as 0.3683 g/g by Ren *et al.* (2011)), K_L is the Langmuir isotherm constant (reported as 0.047 L/mg by Ren *et al.* (2011)), and C_e is the equilibrium concentration of QAC after 4 h. Ren *et al.* (2011) also carried out kinetic studies to characterize QAC adsorption over time. The kinetics of QAC adsorption onto activated sludge were found to be best described by Ren *et al.* (2011) with a pseudo-second-order kinetic expression (Equation (5)):

$$\frac{dq_t}{dt} = k(q_e - q_t)^2 \quad (5)$$

where q_t is the sorbed phase QAC concentration at time t . The final adsorption rate equation used for this study (Equation (6)) combined the isotherm and second-order kinetic expressions described above accounting for the

appropriate unit conversions:

$$\text{Rate}_{\text{ads}} = \frac{1000}{\text{TSS}} \cdot k \cdot \left(q_{\text{max}} \times 0.988^{(T-15)} \cdot \frac{K_L \cdot C_e}{1 + K_L \cdot C_e} - \frac{C_{\text{ads}}}{\text{TSS}} \right)^2 \quad (6)$$

where 1,000 is a units conversion constant (mg/g), C_{ads} is the concentration of adsorbed QAC, and k is the adsorption rate constant.

The overall mathematical model was incorporated as an add-on model in the BioWin 5.3 wastewater treatment process simulator using BioWin's Model Builder functionality. Table 1 outlines the processes and associated kinetic rate equations developed for this model. The concentration of liquid phase QAC is denoted as C_i . Table 2 outlines the associated stoichiometry matrix for each of the processes described in Table 1. The rate and stoichiometric constants are summarized in Table 3. The rate constants were based on data provided in the literature or derived via comparison of the model predictions to measured data in the literature.

RESULTS AND DISCUSSION

Both the acclimated bench-scale BNR system utilized by Hajaya (2011) and the non-acclimated batch system utilized by Yang *et al.* (2014) were configured and simulated in BioWin 5.3 using the reported operational parameters. The observations noted from experimentation were used for calibration of the model developed in this study, not for comparison between the literature studies.

Hajaya (2011) reported performance results from the BNR system during continuous operation with poultry processing wastewater containing QACs. Table 4 summarizes the measured *versus* predicted performance results from the last reactor (R3) and the effluent of the BNR system (see Figure 1). The predicted results were obtained via steady state simulations. The modeled parameters are within the same range as the measured values. There are some minor deviations; likely these are due to some uncertainty around the detailed wastewater characteristics. In addition, the parameters reported by Hajaya were averaged during continuous operation with slight variations at different QAC target concentrations in the influent while the simulated results were obtained with constant QAC target concentrations of 5, 10, 15, 45 and 60 mg QAC/L.

Hajaya (2011) reported the steady state QAC concentrations throughout the BNR system (Figure 1) during operation with step-increased influent QAC concentrations

Table 1 | Summary of process rate equations for all processes

No.	Biological process	Reaction rates
1	AOB growth with Ci inhibition	$MuMax_{AOB} \cdot ThetaMuaob^{T-20} \cdot \frac{Kiaob}{Ci + Kiaob} \cdot \frac{DO}{K_{oaob} + DO} \cdot \frac{NH_3N}{K_{aob} + NH_3N} \cdot \frac{CO_2}{K_{sCO_2} + CO_2} \cdot \frac{PO_4-P}{P04P_{limit} + PO_4-P} \cdot Z_{AOB} \cdot pHinhibition$
2	NOB growth with Ci inhibition	$MuMax_{NOB} \cdot ThetaMunob^{T-20} \cdot \frac{Kinob}{Ci + Kinob} \cdot \frac{DO}{K_{onob} + DO} \cdot \frac{NO_2-N}{K_{nO_2} + NO_2-N} \cdot \frac{CO_2}{K_{CO_2} + CO_2} \cdot \frac{PO_4-P}{P04P_{limit} + PO_4-P} \cdot Z_{NOB} \cdot pHinhibition$
3	Aerobic growth of OHO on Ci	$HMuCiMax \cdot Thetaboho^{T-20} \cdot \frac{Ci}{Ci + Ksioho + \frac{Ci^2}{Kioho}} \cdot \frac{DO}{SWHetroAirOnOff + DO} \cdot \frac{NH_3N}{SWNH3_limit + NH_3N} \cdot \frac{PO_4-P}{SWPGro_limit + PO_4-P} \cdot Z_{BH} \cdot pHinhibition$
4	Anoxic growth of OHO on Ci with NO ₃ N → NO ₂ -N	$HMuCiMax \cdot Thetaboho^{T-20} \cdot \frac{Ci}{Ci + Ksioho + \frac{Ci^2}{Kioho}} \cdot \frac{SWHetroAirOnOff}{SWHetroAirOnOff + DO} \cdot \frac{SWNH3_limit}{SWNH3_limit + NH_3N} \cdot \frac{NO_3-N}{SWAnoxicOnOff + NO_3-N} \cdot \frac{PO_4-P}{SWPGro_limit + PO_4-P} \cdot Z_{BH} \cdot \sigma_{ANX} \cdot pHinhibition$
5	Anoxic growth of OHO on Ci with NO ₂ N	$HMuCiMax \cdot Thetaboho^{T-20} \cdot \frac{Ci}{Ci + Ksioho + \frac{Ci^2}{Kioho}} \cdot \frac{SWHetroAirOnOff}{SWHetroAirOnOff + DO} \cdot \frac{SWNH3_limit}{SWNH3_limit + NH_3N} \cdot \frac{NO_2-N}{SWAnxNO2OnOff + NO_2-N} \cdot \frac{PO_4-P}{SWPGro_limit + PO_4-P} \cdot Z_{BH} \cdot \sigma_{ANX} \cdot pHinhibition$
6	Anoxic growth of OHO on Ci with NO ₃ N → N ₂	$HMuCiMax \cdot Thetaboho^{T-20} \cdot \frac{Ci}{Ci + Ksioho + \frac{Ci^2}{Kioho}} \cdot \frac{SWHetroAirOnOff}{SWHetroAirOnOff + DO} \cdot \frac{SWNH3_limit}{SWNH3_limit + NH_3N} \cdot \frac{NO_3-N}{SWAnoxicOnOff + NO_3-N} \cdot \frac{PO_4-P}{SWPGro_limit + PO_4-P} \cdot Z_{BH} \cdot \sigma_{ANX} \cdot pHinhibition$
7	Aerobic growth of OHO on COD with Ci inhibition	$HMuMax \cdot Thetaboho^{T-20} \cdot \frac{Kioho}{Ci + Kioho} \cdot \frac{COD}{K_{sCOD} + COD} \cdot \frac{DO}{SWHetroAirOnOff + DO} \cdot \frac{NH_3N}{SWNH3_limit + NH_3N} \cdot \frac{PO_4-P}{SWPGro_limit + PO_4-P} \cdot \frac{Z_{BH}}{(HKsCOD + Sbsa + Sbsp + Sbsc + Ci)} \cdot Sbsc \cdot pHinhibition$
8	Anoxic growth of OHO on COD with Ci inhibition with NO ₃ N → NO ₂ -N	$HMuMax \cdot Thetaboho^{T-20} \cdot \frac{Kioho}{Ci + Kioho} \cdot \frac{COD}{HKsCOD + COD} \cdot \frac{SWHetroAirOnOff}{SWHetroAirOnOff + DO} \cdot \frac{SWNH3_limit}{SWNH3_limit + NH_3N} \cdot \frac{NO_3-N}{SWAnoxicOnOff + NO_3-N} \cdot \frac{PO_4-P}{SWPGro_limit + PO_4-P} \cdot \frac{Z_{BH}}{(HKsCOD + Sbsa + Sbsp + Sbsc + Ci)} \cdot Sbsc \cdot \sigma_{ANX} \cdot pHinhibition$

(continued)

Table 1 | continued

No.	Biological process	Reaction rates
9	Anoxic growth of OHO on COD with Ci inhibition with NO ₂ -N	$HMuMax \cdot Thetaboho^{T-20} \cdot \frac{Kioho}{Ci + Kioho} \cdot \frac{COD}{HKsCOD + COD} \cdot \frac{SWHetroAirOnOff}{SWHetroAirOnOff + DO} \cdot \frac{SWNH3_limit}{SWNH3_limit + NH_3N} \cdot \frac{NO_2-N}{SWAnxNO2OnOff + NO_2-N}$ $\frac{PO_4-P}{SWPGro_limit + PO_4-P} \cdot \frac{Z_{BH}}{(HKsCOD + Sbsa + Sbsp + Spsc + Ci)} \cdot Spsc \cdot \sigma_{ANX} \cdot pHinhibition$
10	Anoxic growth of OHO on COD with Ci inhibition with NO ₃ -N → N ₂	$HMuMax \cdot Thetaboho^{T-20} \cdot \frac{Kioho}{Ci + Kioho} \cdot \frac{COD}{HKsCOD + COD} \cdot \frac{SWHetroAirOnOff}{SWHetroAirOnOff + DO} \cdot \frac{SWNH3_limit}{SWNH3_limit + NH_3N} \cdot \frac{NO_2-N}{SWAnxNO2OnOff + NO_2-N}$ $\frac{PO_4-P}{SWPGro_limit + PO_4-P} \cdot \frac{Z_{BH}}{(HKsCOD + Sbsa + Sbsp + Spsc + Ci)} \cdot Spsc \cdot \sigma_{ANX} \cdot pHinhibition$
11	Adsorption of QAC to biomass	$\frac{1000}{TSS} \cdot kads \cdot \left(qmax \cdot \frac{ThetaAds^{T-15}}{1 + KL \cdot Ci} \cdot \frac{KL \cdot Ci}{1 + KL \cdot Ci} \cdot \frac{Cads}{TSS} \right)^2$

(from day 33 to 381 of the experiment). Figure 2 illustrates the measured versus modelled QAC concentrations through the BNR system at QAC feed concentrations of 5, 10, 15, 45 and 60 mg/L. Note that, in Figure 2, the bars for measured data represent the average QAC concentration, and the error bars represent the standard deviation of the measurements. The concentration of QAC is the bulk liquid value; this is a consequence of the influent QAC mass rate and the adsorption/biodegradation rates of QAC in the process (each of which depend on the biomass inventory or SRT of the system). The amount of QAC adsorption to solids was calibrated based on non-active solid concentrations in the pre-anoxic (R1) reactor (since RAS is discharged to the anoxic (R2) reactor), and the amount of QAC removal in R1. Due to adsorption and anoxic growth in the pre-anoxic (R1) and anoxic (R2) reactors, the QAC concentration was always below 2 mg/L in the aerobic reactor (R3); therefore, no impact on nitrification was observed. The modeled results compare favorably with the measured concentrations at all of the feed concentrations tested. Therefore, the model does a reasonable job of predicting QAC adsorption and aerobic/anoxic biodegradation by OHOs.

The experimental nitrification results reported by Yang et al. (2014) were used to test the predicted nitrification performance of the mathematical model. The short-term nitrification assays by Yang et al. (2014) show the effect of QAC on the removal rate of 100 mg NH₄-N/L at 20 °C. The simulations were conducted with constant QAC concentration throughout the test as was the case in the experiments. The simulation results of the short term nitrification assays are illustrated in Figure 3. The lines in Figure 3 represent the modeled N species results; the points represent the measured N species results reported in Yang et al. (2014). In the experiments, QAC was observed to inhibit nitrification at a liquid phase concentration of 2 mg/L, as indicated by (1) a low ammonia removal rate and (2) no nitrite accumulation (which indicates a lower than typical AOB growth rate (Dold et al. 2015). Figure 3(a) (top chart) shows the N species results when a QAC concentration of 2 mg/L was applied. With a QAC concentration of 2 mg/L, most of the ammonia is oxidized in 48 h and no nitrite accumulation is observed. This low ammonia removal rate and lack of nitrite accumulation indicates a degree of AOB inhibition. Figure 3(b) (bottom chart) shows the N species results when a QAC concentration of 10 mg/L was applied. Ammonia only is reduced from 95 mg/L to 62 mg/L in 96 h. This very low ammonia removal rate and lack of nitrite accumulation indicates

Table 2 | Summary of process stoichiometry

Process	Zbh	Zaob	Znob	Sbsc	NH ₃ N	NO ₂ N	NO ₃ -N	N ₂	PO ₄ -P	SCO ₂	Cads	Ci	DO
1		1			-fnaob - 1/Yaob	1/Yaob			-fpaob	-1/32			-(3.43-Yaob)/ Yaob
2			1		-fnnob	-1/Ynob	1/Ynob		-fpnob	-1/33			-(1.14-Ynob)/ Ynob
3	1				-HFzbn				-HFzbp	(1-Yh_Ci_Aer)/ (Yh_Ci_Aer* MWOxygen2)	-1/ Yh_ Ci_Aer		-(1-Yh_Ci_Aer)/ Yh_Ci_Aer
4	1				-HFzbn	(1-Yh_Ci_Anox)/ (gOD_NO3toNO2* Yh_Ci_Anox)	-(1-Yh_Ci_Anox)/ (gOD_NO3toNO2* Yh_Ci_Anox)		-HFzbp	(1-Yh_Ci_Anox)/ (Yh_Ci_Anox* MWOxygen2)	-1/ Yh_Ci_ Anox		
5	1				-HFzbn	(-1-Yh_Ci_Anox)/ (gOD_NO2toN2* Yh_Ci_Anox))		(1-Yh_Ci_Anox)/ (gOD_NO2toN2* Yh_Ci_Anox)	-HFzbp	(1-Yh_Ci_Anox)/ (Yh_Ci_Anox* MWOxygen2)	-1/Yh_ Ci_Anox		
6	1				-HFzbn		-(1-Yh_Ci_Anox)/ (gOD_NO3toN2* Yh_Ci_Anox)	(1-Yh_Ci_Anox)/ (gOD_NO3toN2* Yh_Ci_Anox)	-HFzbp	(1-Yh_Ci_Anox)/ (Yh_Ci_Anox* MWOxygen2)	-1/ Yh_ Ci_Anox		
7	1			-1/Yh_ Sbsa_ Aer	-HFzbn				-HFzbp	(1-Yh_Cs_Aer)/ (Yh_Cs_Aer* MWOxygen2)			-(1-Yh_Cs_Aer) /Yh_Cs_Aer
8	1			-1/Yh_ Sbsa_ Anox	-HFzbn	(1-Yh_Cs_Anox)/ (gOD_NO3toNO2* Yh_Cs_Anox)	-(1-Yh_Cs_Anox)/ (gOD_NO3toNO2* Yh_Cs_Anox)		-HFzbp	(1-Yh_Cs_Anox)/ (Yh_Cs_Anox* MWOxygen2)			
9	1			-1/Yh_ Sbsa_ Anox	-HFzbn	-(1-Yh_Cs_Anox)/ (gOD_NO2toN2* Yh_Cs_Anox)		(1-Yh_Cs_Anox)/ (gOD_NO2toN2* Yh_Cs_Anox)	-HFzbp	(1-Yh_Cs_Anox)/ (Yh_Cs_Anox* MWOxygen2)			
10	1			-1/Yh_ Sbsa_ Anox	-HFzbn		-(1-Yh_Cs_Anox)/ (gOD_NO3toN2* Yh_Cs_Anox)	(1-Yh_Cs_Anox)/ (gOD_NO3toN2* Yh_Cs_Anox)	-HFzbp	(1-Yh_Cs_Anox)/ (Yh_Cs_Anox* MWOxygen2)			
11											1	-1	

Table 3 | Summary of rate and stoichiometric constants

Parameter	Value	Parameter	Value
Rate constants			
MuMax _{AOB}	0.9	MuMax _{NOB}	0.7
ThetaMu _{AOB}	1.072	ThetaMu _{NOB}	1.06
K _{DOAOB}	0.25	K _{DONOB}	0.5
K _{AOB}	0.7	K _{NOB}	0.1
K _{iAOB}	1.39	K _{iNOB}	200
HMuCiMax	0.26	SWNH3_limit	0.005
Thetab _{OHO}	1.029	SWPGro_limit	0.001
Ksi _{OHO}	10	SWHeteroAirOnOff	0.05
Ki _{OHO}	20	SWAnoxicOnOff	0.1
NO3_Ratio	0.4	SWAnoxNO2OnOff	0.01
NO2_Ratio	0.6	Ks _{CO2}	0.1
HKsCOD	5	ThetaAds	0.9884
HMuMax	3.2	KL	0.047
Kads	5	qmax	0.36
Stoichiometric constants			
Y _{AOB}	0.15	Y _{NOB}	0.09
fn _{AOB}	0.07	fn _{NOB}	0.07
fp _{AOB}	0.022	fp _{NOB}	0.022
HFzbp	0.022	Yh_Cs_Anox	0.53
HFzbn	0.07	Yh_Cs_Aer	0.666
Yh_Ci_anox	0.53	Yh_Sbsa_Aer	0.67
Yh_Ci_aer	0.666	Yh_Sbsa_Anox	0.53
gOD_NO3toNO2	1.142	gOD_NO3toN2	2.8556
gOD_NO2toN2	1.713	MWOxygen2	31.998

more severe degree of AOB inhibition. Based on these results, the model accurately predicts the inhibitory threshold of 2 mg/L for AOB conversion of ammonia to nitrite. It is worth noting that the authors' literature search

did not reveal data suitable for accurately quantifying NOB inhibition kinetics. However, the model has been structured in a way to allow for NOB inhibition if required/desired.

Table 4 | Comparison of measured versus modeled performance parameters

Parameter	R ₃		Effluent	
	Measured	Modeled	Measured	Modeled
pH	7.0 ± 0.4	7.1	7.0 ± 0.4	7.1
TSS (mg/L)	1,309 ± 124	1,390	52 ± 2	42
VSS (mg/L)	1,073 ± 80	1,180	42 ± 2	37
Soluble COD (mg/L)	273 ± 74	268	282 ± 15	268
NH ₃ (mg N/L)	0.9 ± 0.2	0.7	1 ± 0.5	0.7
NO ₃ (mg N/L)	23 ± 5	25.5	20 ± 7	25.5
NO ₂ (mg N/L)	1.9 ± 0.9	0.2	1 ± 4	0.2

CONCLUSION

A mechanistic mathematical model to describe the fate of QACs in activated sludge processes was developed as an add-on model in BioWin 5.3. The model includes removal of QACs via both biodegradation and adsorption, and quantifies the degree of QAC inhibition on the growth of AOBs, NOBs and OHOs. The model assumes that microorganisms are already acclimated to QACs; no population shifts or changes in metabolic abilities are modeled with time. Simulation results were compared to the studies of Hajaya (2011) and Yang et al. (2014) as a means of calibration. The model

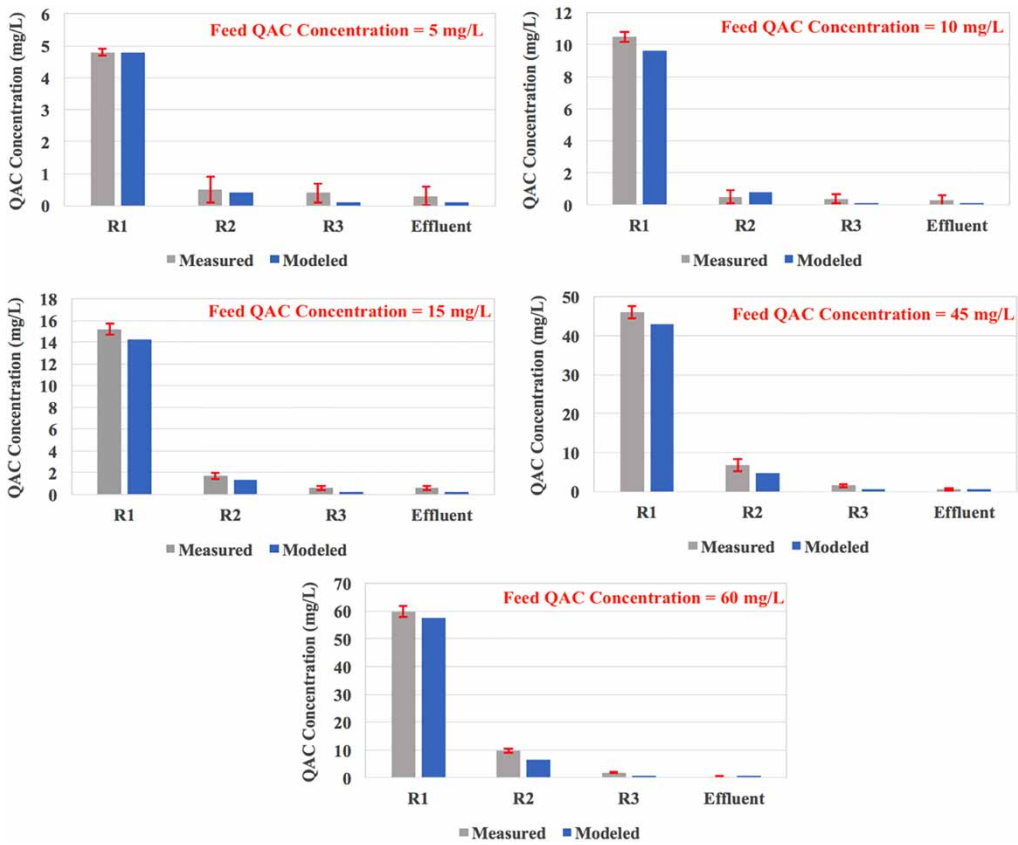


Figure 2 | Measured versus modeled QAC concentrations through the BNR system in Hajaya's study at QAC feed concentrations of 5, 10, 15, 45 and 60 mg/L.

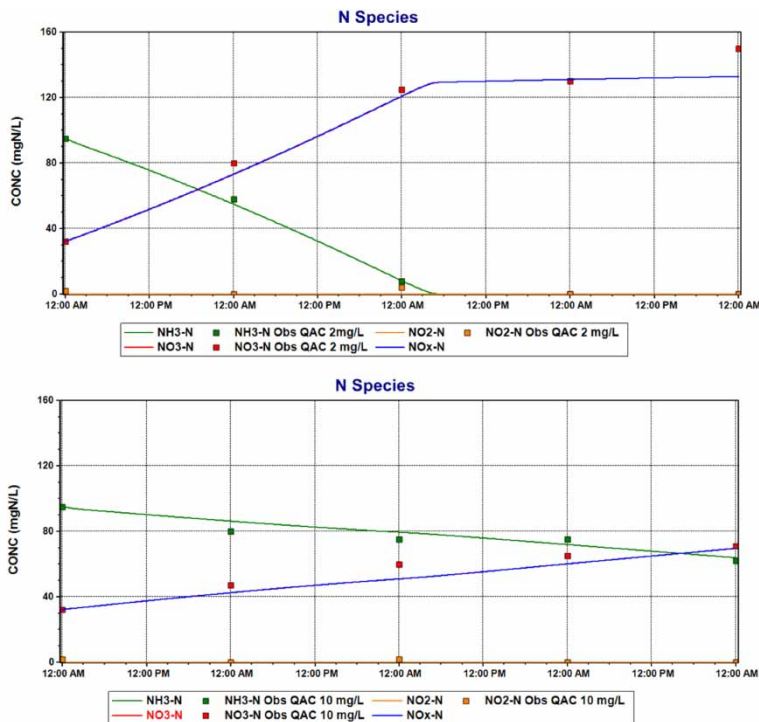


Figure 3 | Measured versus modeled N species responses for Yang et al. (2014) short-term nitrification bioassays at QAC batch concentrations of 2 and 10 mg/L.

was found to accurately predict the inhibition of nitrification in batch bioassays and the concentration of QAC in the bulk liquid of a laboratory-scale BNR activated sludge system.

The model provides a preliminary framework for simulating the potential impacts of inhibitory substances on BNR WWTP performance. The following important processes are taken into account by the model:

- Adsorption of QACs onto the biological sludge mass, thereby reducing the potential for inhibition.
- Aerobic and anoxic growth of heterotrophic organisms on QACs according to Haldane kinetics.
- Aerobic and anoxic growth of heterotrophic organisms on soluble influent COD inhibited by the presence of QACs using a Monod-type rate reduction if QACs are present.
- Inhibition of ammonia and nitrite oxidizing organisms using a Monod-type rate reduction if QACs are present.

The model presented here should be viewed as a first step in developing a more comprehensive biological model incorporating inhibition kinetics. Aspects for future investigation could include the following:

- Refinement of the split between adsorption and biodegradation of QACs as removal pathways.
- Refinement of the model to include acclimation of heterotrophic biomass to QACs (e.g. incorporating two populations of heterotrophic biomass [one population that grows slowly on both other COD and QAC in the presence of QAC, and a second specialist population that has a relatively higher growth rate on QAC but can **only** grow on QAC]; using a single population of heterotrophic biomass with a growth rate that changes as a function of the amount of time exposed to QACs).
- Impact of QACs on NOB kinetics.
- Impact of QACs on organisms responsible for biological excess phosphorus removal.
- Impact of temperature on inhibition coefficients.

REFERENCES

- Aiba, S., Shoda, M. & Nagatani, M. 1968 Kinetics of product inhibition in alcohol fermentation. *Biotechnology & Bioengineering* **10** (6), 845–864.
- Carbajo, J. B., Petre, A. L., Rosal, R., Berna, A., Leton, P., Garcia-Calvo, E. & Perdigon-Melon, J. A. 2015 Ozonation as pre-treatment of activated sludge process of a wastewater containing benzalkonium chloride and NiO nanoparticles. *Chemical Engineering Journal* **283**, 740–749.
- Chen, M., Zhang, X., Wang, Z., Liu, M., Wang, L. & Wu, Z. 2018 Impacts of quaternary ammonium compounds on membrane bioreactor performance: acute and chronic responses of microorganisms. *Water Research* **134**, 153–161.
- Dold, P. L., Du, W., Burger, G. & Jimenez, J. 2015 Is Nitrite-Shunt Happening in the System? Are NOB Repressed? In: *WEFTEC Conference Proceedings*, Chicago, Illinois.
- Hajaya, M. 2011 *Fate and Effect of Quaternary Ammonium Antimicrobial Compounds on Biological Nitrogen Removal within High-Strength Wastewater Treatment Systems*. PhD Thesis, Georgia Institute of Technology, Atlanta, GA, USA.
- Hajaya, M. G. & Pavlostathis, S. G. 2012 Modeling the fate and effect of benzalkonium chlorides in a continuous-flow biological nitrogen removal system treating poultry processing wastewater. *Bioresource Technology* **130**, 278–287.
- Khan, A. H., Topp, E., Scott, A., Sumarah, M., Macfie, S. M. & Ray, M. B. 2015 Biodegradation of benzalkonium chlorides singly and in mixtures by a *Pseudomonas* sp. isolated from returned activated sludge. *Journal of Hazardous Materials* **299**, 595–602.
- Ren, R. L., Liu, D., Li, K., Sun, J. & Zhang, C. 2011 Adsorption of quaternary ammonium compounds onto activated sludge. *Journal of Water Resource and Protection* **3** (2), 105–113.
- Ruan, T. S., Song, S., Wang, T., Liu, R., Lin, Y. & Jiang, G. 2014 Identification and composition of emerging quaternary ammonium compounds in municipal sewage sludge in China. *Environmental Science & Technology* **48** (8), 4289–4297.
- Sütterlin, H. A., Alexy, R., Coker, A. & Kümmerer, K. 2008 Mixtures of quaternary ammonium compounds and anionic organic compounds in the aquatic environment: elimination and biodegradability in the closed bottle test monitored by LC-MS/MS. *Chemosphere* **72** (3), 479–484.
- Tezel, U. 2009 *Fate and Effect of Quaternary Ammonium Compounds in Biological Systems*. PhD Thesis, Georgia Institute of Technology, Atlanta, GA, USA.
- Yang, J., Tezel, U., Li, K. & Pavlostathis, S. G. 2014 Prolonged exposure of mixed aerobic cultures to low temperature and benzalkonium chloride affect the rate and extent of nitrification. *Bioresource Technology* **179**, 193–201.
- Zhang, C., Tezel, U., Li, K., Liu, D., Ren, R., Du, J. & Pavlostathis, S. G. 2010 Evaluation and modeling of benzalkonium chloride inhibition and biodegradation in activated sludge. *Water Research* **45** (3), 1238–1246.
- Zhang, C., Cui, F., Zeng, G. M., Jiang, M., Yang, Z. Z., Yu, Z. G., Zhu, M. Y. & Shen, L. Q. 2015 Quaternary ammonium compounds (QACs): a review on occurrence, fate and toxicity in the environment. *Science of The Total Environment* **518–519**, 352–362.

First received 27 June 2018; accepted in revised form 16 October 2018. Available online 24 October 2018